

Sinoite ($\text{Si}_2\text{N}_2\text{O}$): Crystallization from EL chondrite impact melts

ALAN E. RUBIN

Institute of Geophysics and Planetary Physics, University of California, Los Angeles, California 90095-1567, U.S.A.

ABSTRACT

Sinoite ($\text{Si}_2\text{N}_2\text{O}$) was previously observed only in EL6 chondrites and recently modeled as having formed over geologic time scales at metamorphic temperatures of ~ 950 °C. I found several ~ 10 – 210 μm -sized subhedral and euhedral grains of twinned, optically zoned sinoite associated with euhedral enstatite and euhedral graphite within impact-melted portions of QUE94368, the first EL4 chondrite. The presence of sinoite within a type 4 chondrite mitigates against the metamorphic model of sinoite formation; it seems more likely that sinoite crystallized from a liquid. During impact melting of EL material, N_2 may have been released from lattice defects in sulfides whereupon it reacted with reduced Si dissolved in the metallic Fe-Ni melt and with fine-grained or molten silica derived from the silicate fraction of the EL assemblage. The N that formed the sinoite was derived from the silicate melt or from temporary, melt-filled cavities constructed from unmelted EL material in which the nitrogen fugacity may have reached ~ 40 to 130 bars (0.004 to 0.013 GPa). Sinoite in EL6 chondrites may have formed either metamorphically, as previously proposed, or by means of crystallization from an impact melt, as in QUE94368. In the latter case, sinoite-bearing EL6 chondrites would be annealed impact-melt breccias.

INTRODUCTION

Natural silicon oxynitride ($\text{Si}_2\text{N}_2\text{O}$) was first observed but not identified by Lacroix (1905) in two EL6 chondrites. It was identified by Andersen et al. (1964) and Keil and Andersen (1965a, 1965b) in several EL6 chondrites where it occurs as ≤ 200 μm -sized euhedral, lath-like grains associated with metallic Fe-Ni and enstatite. The new orthorhombic mineral was named sinoite, an acronym of its chemical formula.

The origin of sinoite is controversial. Herndon and Suess (1976) and Sears (1980) suggested that sinoite is a nebular phase, formed by condensation at high temperatures and pressures from a gas of solar composition. However, more recent thermodynamic calculations (e.g., Larimer and Bartholomay 1979; Fegley 1983) disputed this. For example, Fegley (1983) found that the thermodynamic activities of silicon oxynitride were reduced significantly by the prior condensation of more stable Si-bearing species, making it unlikely that sinoite could form as an equilibrium product from a gas of solar composition. Petaev and Khodakovskiy (1986) and Fogel et al. (1989) proposed that sinoite formed metamorphically at temperatures appreciably below that of the laboratory synthesis of silicon oxynitride (1450 °C; Brosset and Idrestedt 1964). Muenow et al. (1992) suggested that sinoite formed at EL6 metamorphic temperatures (i.e., ~ 950 °C; Muenow et al. 1992; Wasson et al. 1994) over geologic time scales under conditions wherein Si-bearing metallic Fe-Ni acted as a catalyst.

Below, I report the first occurrence of sinoite outside EL6 chondrites. It occurs in QUE94368, a 1.2 g enstatite

chondrite found at $84^\circ 35' 58.4482''\text{S}$, $162^\circ 11' 16.6142''\text{W}$ in the Queen Alexandra Range of Victoria Land, Antarctica, in 1994. The meteorite was classified initially by McBride and Mason (1996) as an E5 chondrite, but, as I show below, QUE94368 is the first EL4 chondrite. It is of weathering class C (McBride and Mason 1996), implying severe surface rustiness and pervasive terrestrial oxidation of metal particles.

ANALYTICAL PROCEDURES

Polished thin section QUE94368,4, obtained from the NASA Johnson Space Center in Houston, was studied microscopically using transmitted and reflected light. Minerals were analyzed with the UCLA automated Cameca Camebax-microbeam electron microprobe using crystal spectrometers, a sample current of ~ 12 nA at 15 kV and analysis times of 20 s. PAP corrections were applied to the data. A lead stearate crystal was used to scan for O and N peaks in sinoite. For O, 400 points were scanned at a sample current of 2.2 nA at 15 kV; for N, 20 points were scanned at 1.2 nA and 15 kV.

RESULTS

Petrologic characteristics of QUE94368

QUE94368 consists of enstatite, olivine, sinoite, kamacite, schreibersite, graphite, troilite, rare grains of ferroan alabandite, and goethite (formed by terrestrial weathering of kamacite). Olivine constitutes ~ 0.2 vol% of QUE94368,4; it is rare but definitely present in the Smithsonian library section of QUE94368 (T.J. McCoy, personal communication). Schreibersite occurs typically

as 2–5 μm -sized patches at kamacite-silicate grain boundaries.

The rock contains moderately recrystallized chondrules (Fig. 1a) with fine-grained, silicic-feldspathic mesostases. Chondrules range in apparent diameter from 220 to 1100 μm and average ~ 520 μm ($n = 15$). One 1020×1180 μm -sized porphyritic olivine-pyroxene chondrule is present; this chondrule contains 20–100 μm -sized forsterite grains ($\text{Fa}_{0.19 \pm 0.05}$) poikilitically enclosed in enstatite phenocrysts (Fig. 1b).

Approximately 10–15 vol% of the rock consists of regions containing numerous grains of euhedral enstatite (0.5×7 μm – 30×170 μm) surrounded by kamacite (Fig. 1c) and goethite. The euhedral enstatite grains are moderately more ferroan than most enstatite phenocrysts in intact chondrules ($\text{Fs}_{0.57}$ vs. $\text{Fs}_{0.34}$; Table 1). Whereas most enstatite grains in chondrules contain curvilinear trails of tiny kamacite blebs, such trails are essentially absent in the euhedral enstatite grains. Rubin and Scott (1997) showed that very similar euhedral enstatite grains are abundant in Abee and other EH chondrite impact-melt breccias and virtually absent in unmelted EH chondrites. In Abee some of the euhedral enstatite grains have nucleated on the surfaces of partly resorbed chondrules.

Also present in the same regions of QUE94368 that contain euhedral enstatite grains are abundant euhedral laths of graphite (4×34 μm – 16×150 μm ; Fig. 1c), a few of which possess pyramidal terminations. The euhedral graphite grains are very similar to those in the Abee, Y-791790, and Y-791810 EH impact-melt breccias (Rubin and Scott 1997) as well as those in the weakly shocked ureilites ALHA78019 and Nova 001 (Berkley and Jones 1982; Treiman and Berkley 1994). Similar primary igneous graphite occurs as a rare phase in terrestrial ultramafic xenoliths within alkali basalt (e.g., Figs. 5–7 of Kornprobst et al. 1987).

Graphite also occurs in QUE94368 as ~ 15 μm -diameter aggregates within kamacite; whereas most of the graphite in these aggregates is fine-grained, 10–40% of it occurs as smooth, relatively homogeneous patches that appear to have partly recrystallized.

Sinoite

Sinoite occurs as highly birefringent grains within the euhedral-enstatite- and euhedral-graphite-bearing portions of thin section QUE94368,4; it is also present in the Smithsonian library section (T.J. McCoy, personal communication). In section QUE94368,4, one 50 μm anhedral sinoite grain is adjacent to one end of a 27×140 μm euhedral enstatite grain; a smaller (6×12 μm) subhedral sinoite grain is adjacent to the other end of the same euhedral enstatite grain. Most of the sinoite in this section occurs in a multi-grain cluster of 70–210 μm -sized, mainly rectangular, euhedral grains with distinct optical zoning (Fig. 1d–1f). Although separated, some of the grains in the cluster appear as if they could fit together. The sinoite cluster is adjacent to euhedral enstatite grains and is surrounded by kamacite and goethite (Fig. 1d).

Enclosed within these sinoite grains are smaller (typically 6×20 μm) euhedral, lath-like sinoite crystals that appear to have crystallized at earlier stages from the melt (Fig. 1e). Their continued observability presumably indicates some discontinuity in sinoite crystallization history and might reflect slight differences in composition (e.g., because of the incorporation of impurities). A few of the optically zoned sinoite grains have congruent bands of differing birefringence immediately beneath the grain edge (Fig. 1f); whereas these bands also may indicate discontinuities in crystallization, it is possible that they are an artifact of thin section preparation. Although optically observable twinning is rare in orthorhombic crystals (aragonite is a notable exception), many of the sinoite grains in QUE94368 are twinned (Fig. 1d–1f). Although the twinning probably results from late-stage mutual interference between growing crystals, post-formation shock-induced twinning cannot be ruled out.

Wavelength scans using a lead stearate crystal across the theoretical peaks for O and N on the largest sinoite grains (Fig. 2) indicate the presence of abundant O and N in the mineral. Along with abundant Si determined with a TAP crystal, these peaks identify the mineral in QUE94368 as sinoite.

DISCUSSION

Classification of QUE94368

QUE94368 is not a type 3 chondrite because it lacks very sharply defined chondrules, does not contain glassy chondrule mesostases, and has relatively homogeneous Ca-poor pyroxene compositions (Table 1). Its moderately distinct chondritic structure is characteristic of a type 4 chondrite (Fig. 1a). Approximately 0.2 vol% olivine is present. Because olivine is absent in some type 4 and all type 5 and type 6 enstatite chondrites (Binns 1967; Rubin et al. 1997), I classify QUE94368 as type 4.

Characteristics indicating that QUE94368 is an EL chondrite include: (1) The presence of kamacite with relatively low Si (0.5–0.7 wt%; McBride and Mason 1996), more similar to that in EL chondrites (~ 1 wt%) than that in EH chondrites (~ 3 wt%; Keil 1968); (2) The absence of niningerite and the occurrence of rare grains of ferroan alabandite (this study), {EL chondrites of all petrologic types contain ferroan alabandite [(Mn,Fe)S] and lack niningerite [(Mg,Fe)S], whereas EH3-5 chondrites contain niningerite and lack ferroan alabandite (e.g., Keil 1968; Prinz et al. 1984; Lin et al. 1991; El Goresy et al. 1992)}; and (3) The presence of chondrules with an average apparent diameter of ~ 520 μm (this study). This average is very close to the mean apparent diameter of chondrules in the ALH85119, MAC88136, and PCA91020 EL3 chondrites (~ 550 μm ; A.E. Rubin, unpublished data) and appreciably greater than that of EH3 chondrules (~ 220 μm ; Rubin and Grossman 1987). Thus, QUE94368 is the first known EL4 chondrite, completing the EL3-EL6 metamorphic sequence (cf. Rubin et al. 1997).

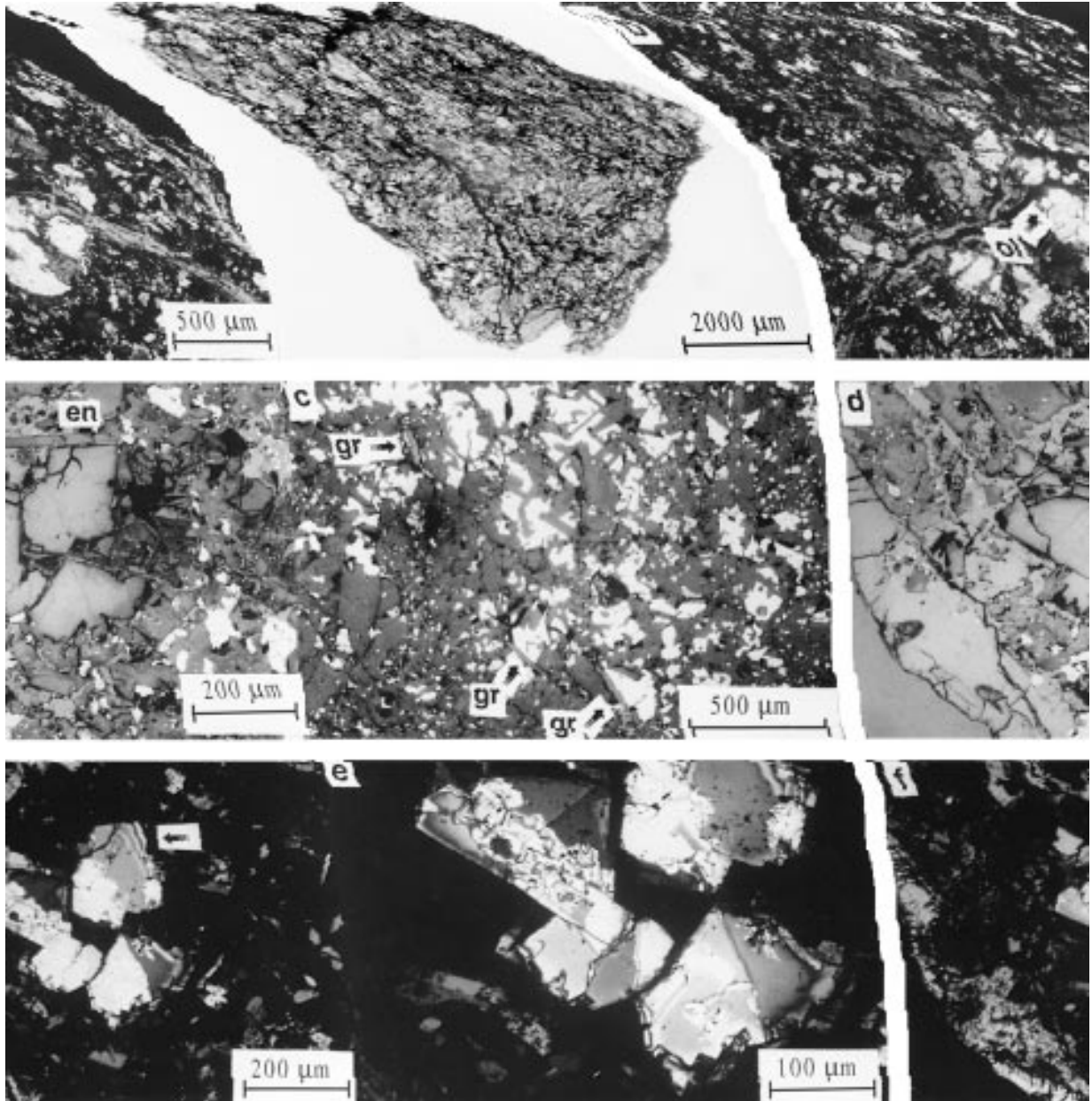


FIGURE 1. Photomicrographs of QUE94368. (a) Whole thin section view of QUE94368,4 showing discernible but moderately recrystallized chondrules. A large goethite-rich weathering vein (black) cuts across the section mainly from north to south. Transmitted light. (b) Porphyritic olivine-pyroxene chondrule containing 20–100 μm -sized forsterite grains (white; **ol**, arrow) poikilitically enclosed in enstatite phenocrysts (gray). X-nicols. (c) Impact-melted region of the rock containing numerous euhedral enstatite laths (medium gray) as well as a few graphite laths (light gray; **gr**, arrows) surrounded by kamacite (white). Reflected light. (d) Euhedral enstatite lath (**en**) adjacent to a

multi-grain cluster of sinoite grains (medium gray) with visible twin boundaries (medium gray). Light gray material surrounding the enstatite and sinoite is goethite formed by the terrestrial weathering of kamacite. Reflected light. (e) Optical zoning in the cluster of sinoite grains. Some grains contain internal lath-like zones that represent the boundaries of sinoite grains that crystallized from the melt at early stages. X-nicols. (f) Same view as in (d) showing sinoite grain cluster with prominent twinning and congruent bands of differing birefringence beneath the grain edge (arrow). X-nicols.

TABLE 1. Mean compositions and standard deviations (wt%) of enstatite and olivine in QUE94368

	Euhedral enst grains	Enstatite in chondrules	FeO-enriched enst in a chd	Olivine in a chd
No. of grains	8	8	1	2
SiO ₂	60.9 ± 0.4	60.9 ± 0.3	59.8	41.6
Al ₂ O ₃	0.11 ± 0.02	0.15 ± 0.04	0.13	<0.04
Cr ₂ O ₃	<0.04	<0.04	<0.04	<0.04
FeO*	0.40 ± 0.12	0.24 ± 0.08	1.2	0.20
MnO	<0.04	<0.04	0.04	<0.04
MgO	39.0 ± 0.2	38.9 ± 0.4	37.8	58.2
CaO	0.56 ± 0.09	0.57 ± 0.07	0.64	<0.04
Total	101.0	100.8	99.6	100.0
End-member	Fs _{0.57} Wo _{1.0}	Fs _{0.34} Wo _{1.0}	Fs _{1.7} Wo _{1.2}	Fa _{0.19}

Note: enst = enstatite; chd = chondrule.

* Total Fe as FeO.

QUE94368 as an impact-melt breccia

Numerous euhedral enstatite grains, very similar to those that occur in Abee and other EH impact-melt breccias (Rubin and Scott 1997), are concentrated in regions constituting 10–15 vol% of QUE94368. It seems likely that the euhedral enstatite grains in QUE94368 formed in the same manner as those in Abee, and that QUE94368, like Abee, is an impact-melt breccia. The euhedral shapes of the enstatite grains in these rocks were acquired through primary crystallization from a melt, consistent with the high surface energy and high surface-energy anisotropy of orthopyroxene (e.g., Spry 1969). The higher FeO contents of the euhedral enstatite grains in QUE94368 in comparison with most enstatite phenocrysts in chondrules in this rock probably reflect crystallization from a melt slightly enriched in FeO. This enrichment most likely resulted from the impact melting of rare chondrules containing relatively FeO-rich, Ca-poor pyroxene grains (cf. Table 1); for example, a few Ca-poor pyroxene grains in EL3 chondrites contain up to 12 mol% Fs (Score and Mason 1987).

The absence of curvilinear trails of kamacite blebs in the euhedral enstatite grains is consistent with crystallization of euhedral enstatite after the shock event that partly melted QUE94368 and caused extensive silicate darkening in the unmelted portions (cf. Rubin 1992). The sinoite crystals in QUE94368 also lack curvilinear trails of kamacite blebs and, hence, also appear to have crystallized after the main shock event.

The euhedral graphite grains in QUE94368 occur in the same regions as the euhedral enstatite grains. The graphite grains are very similar to those in Abee and are not mainly associated with kamacite. Outside these regions, graphite occurs as aggregates within kamacite just as in unmelted EH chondrites such as Indarch. This occurrence suggests that during the impact events that melted QUE94368 and Abee, graphite-bearing metal was melted and euhedral graphite crystallized as a primary phase separate from the metal.

Origin of sinoite

The presence of sinoite within an olivine-bearing type 4 chondrite, which, by analogy to ordinary chondrites

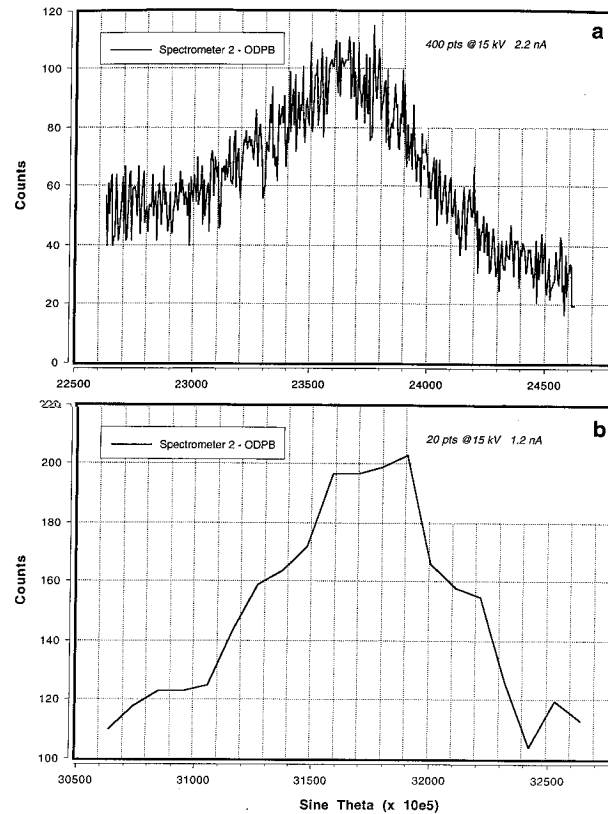


FIGURE 2. Wavelength spectrometer scans of the large sinoite grain (shown at bottom right of Fig. 1e) using a lead stearate crystal. Counts are plotted against $\sin \theta \times 10^5$. (a) O (raw data). In these units, the theoretical O peak is at $\sin \theta = 23874$. (b) N (smoothed curve). In these units, the theoretical N peak is at $\sin \theta = 31939$. In conjunction with the determination with a TAP crystal of abundant Si in the grain, these peaks confirm the identification of the mineral as sinoite.

(Table 4.4 of Dodd 1981), was probably not heated appreciably above 700 °C (except in its impact-melted regions), argues against the metamorphic model for sinoite formation. In contrast, the presence of twinned, optically zoned, euhedral grains of sinoite within impact-melted portions of QUE94368 indicate that sinoite in this rock crystallized from a melt.

N in enstatite chondrites probably occurs mainly within lattice defects in sulfide phases (Muenow et al. 1992). Dynamic high-temperature mass-spectrometric analysis of EH and EL chondrites indicates that N₂⁺ is released between ~950 and 1080 °C (Muenow et al. 1992); this interval corresponds approximately to the temperature of the metallic-Fe-Ni-sulfide cotectic. During the impact melting of EL material, N₂ would be released from sulfide. Some of the N would dissolve in the silicate melt (which can accommodate up to 0.5 wt% N at 1500 °C; Fogel 1994), substituting for O (e.g., Baur 1972).

Although some N₂ probably escaped during the impact event, it seems likely that sufficient amounts were retained for the formation of sinoite because another

N-bearing phase (i.e., osbornite, TiN) was reported in other samples of impact-melted enstatite chondrite material. Kinsey et al. (1995) found 15 μm -sized osbornite grains within an impact-melt rock clast in EL6 Hvittis (although it is absent from the Hvittis matrix). McCoy et al. (1995) reported three 10–20 μm -sized osbornite grains in the Ilafegh 009 EL impact-melt rock and one $15 \times 30 \mu\text{m}$ grain in impact-melted regions of the Happy Canyon EL impact-melt breccia. In all three cases, it seems very likely that osbornite crystallized from the melt.

Sinoite in QUE94368 probably formed in a manner somewhat analogous to the laboratory synthesis of silicon oxynitride (Brosset and Idrestedt 1964): N_2 reacted with reduced Si dissolved in the metallic Fe-Ni melt and with fine-grained (or molten) silica derived from the silicate fraction of the EL chondrite assemblage. At 1400–1500 $^\circ\text{C}$, the following reaction, suggested by Ryall and Muan (1969), may have occurred:



for which ΔG_f° , the free energy of reaction, ranges from approximately -530 to -550 kJ/mol (Fegley 1981). It seems unlikely that sinoite could have formed by a reaction between silica and silicon nitride (i.e., $\text{SiO}_2 + \text{Si}_3\text{N}_4 = 2\text{Si}_2\text{N}_2\text{O}$) because Si_3N_4 in enstatite chondrites occurs as very rare $\leq 2 \mu\text{m}$ -sized grains (Alexander et al. 1994; Lee et al. 1995).

It is unclear if the N_2 that formed the sinoite was derived from the silicate melt or from temporary, melt-filled cavities constructed from unmelted EL material in which relatively high N_2 partial pressures were achieved. The nitrogen fugacity (in atm) in equilibrium with sinoite can be determined from the following equation after Alexander et al. (1994):

$$\log(f_{\text{N}_2}) = (-15011/T) + 8.245 - [1.5 \log(X_{\text{Si}})] - [(17450/T) - 9.45](X_{\text{Si}})$$

where X_{Si} is the mole fraction of Si in kamacite and T is the temperature in kelvins. From the average composition of kamacite in EL chondrites (Table 5 of Keil 1968), X_{Si} can be determined to be ~ 0.026 . For temperatures of 1400 $^\circ\text{C}$ and 1500 $^\circ\text{C}$, the $\log(f_{\text{N}_2})$ values are +1.6 and +2.1, respectively. These values correspond to f_{N_2} values of ~ 40 bars and ~ 130 bars, respectively.

Sinoite-bearing EL6 chondrites

EL6 chondrites that contain sinoite include Forrest 033, Hvittis, Jajh deh Kot Lalu, Pillistfer, Ufana, Yilmia, ALHA81021 (and its paired specimen ALH83018), LEW88714, and EET90102 (Lacroix 1905; Andersen et al. 1964; Keil and Andersen 1965a, 1965b; Buseck and Holdsworth 1972; Rubin et al. 1997; Schwarz and Mason 1983, 1987, 1992; Satterwhite and Mason 1992). The sinoite grains in these rocks range up to 200 μm in length and many have subhedral to euhedral morphologies (e.g., Fig. 1 of Andersen et al. 1964; Fig. 1 of Keil and Andersen 1965a).

Some EL6 chondrites are fragmental or impact-melt

breccias (e.g., Hvittis and Blithfield; Rubin 1983a, 1984; Rubin et al. 1997); others contain clasts or large opaque veins for which an impact origin seems probable (e.g., Atlanta, Eagle and Khairpur; Rubin 1983b; Olsen et al. 1988; Rubin et al. 1997). Jajh deh Kot Lalu contains a $\sim 2 \times 16\text{-mm}$ chondrule-free, oldhamite-rich vein that probably formed by an impact process (Rubin et al. 1997). Because all known EL6 chondrites are shock stage S2 (even though some have been significantly altered by impacts), it seems likely that proto-EL6 material was shocked to S3-S5 levels (and some was impact melted) before peak metamorphism (Rubin et al. 1997); annealing erased many of the shock features in these samples. The rocks were shocked again to stage S2 after metamorphism.

Although it is possible that sinoite in EL6 chondrites formed metamorphically over geologic time scales as suggested by Muenow et al. (1992), a plausible alternative is that sinoite in EL6 chondrites formed in the same manner as sinoite in QUE94368, i.e., by crystallization from an EL chondrite impact melt. This formation is consistent with the euhedral shapes of many of the EL6 sinoite grains and with the inferred shock history of some EL6 chondrites. This alternative leaves open the possibility that the rare euhedral enstatite laths in some sinoite-bearing EL6 chondrites also crystallized from impact melts before metamorphism.

The bulk N contents of enstatite chondrites were measured by several teams of investigators and found to vary from ~ 100 to 1000 $\mu\text{g/g}$ (Moore et al. 1969; Kung and Clayton 1978; Thiemens and Clayton 1983; Grady et al. 1986; Muenow et al. 1992). Although Grady et al. (1986) found no systematic tendency for N content to vary with petrologic type, the data of Moore et al. (1969) indicate that bulk N may be higher in sinoite-bearing EL6 chondrites ($\sim 650\text{--}780 \mu\text{g/g}$) than in EL6 chondrites that lack sinoite ($\sim 50 \mu\text{g/g}$) or in EH chondrites (none of which contain sinoite) ($\sim 180\text{--}430 \mu\text{g/g}$). If this is the case, sinoite formation may be restricted to impact-melted enstatite chondrites that initially possessed abundant bulk N.

ACKNOWLEDGMENTS

I thank K. Keil and W.A. Dollase for discussions, F.T. Kyte, A.L. Sailer, and J.T. Wasson for technical assistance, T.J. McCoy for examining the Smithsonian library section of QUE94368, and the Antarctic Meteorite Working Group for providing thin section QUE94368.4. Helpful reviews were provided by M.K. Weisberg and K. Lodders. This work was supported in part by NASA grant NAGW-5099.

REFERENCES CITED

- Alexander, C.M.O'D., Swan, P., and Prombo, C.A. (1994) Occurrence and implications of silicon nitride in enstatite chondrites. *Meteoritics*, 29, 79–85.
- Andersen, C.A., Keil, K., and Mason, B. (1964) Silicon oxynitride: A meteoritic mineral. *Science*, 146, 256–257.
- Baur, W.H. (1972) Occurrence of nitride nitrogen in silicate minerals. *Nature*, 240, 461–462.
- Berkley, J.L. and Jones, J.H. (1982) Primary igneous carbon in ureilites: Petrological implications. Proceedings of the Lunar and Planetary Science Conference, 13th, A353-A364.
- Binns, R.A. (1967) Olivine in enstatite chondrites. *American Mineralogist*, 52, 1549–1554.

- Brosset, C. and Idrestedt, I. (1964) Crystal structure of silicon oxynitride, $\text{Si}_2\text{N}_2\text{O}$. *Nature*, 201, 1211.
- Buseck, P.R. and Holdsworth, E.F. (1972) Mineralogy and petrology of the Yilmia enstatite chondrite. *Meteoritics*, 7, 429–447.
- Dodd, R.T. (1981) *Meteorites: A Petrologic-chemical Synthesis*, 368 p. Cambridge University Press, Cambridge.
- El Goresy, A., Wadhwa, M., Nagel, H.-J., Zinner, E.K., Janicke, J., and Crozaz, G. (1992) ^{53}Cr - ^{53}Mn systematics of Mn-bearing sulfides in four enstatite chondrites (abstract). *Lunar and Planetary Science*, 23, 331–332.
- Fegley, M.B. (1981) The thermodynamic properties of silicon oxynitride. *Journal of the American Ceramic Society*, 64, C124–C126.
- Fegley, B. (1983) Primordial retention of nitrogen by terrestrial planets and meteorites. Proceedings of the Lunar and Planetary Science Conference, 13th, A853–A868.
- Fogel, R.A. (1994) Nitrogen solubility in aubrite and E chondrite melts (abstract). *Lunar and Planetary Science*, 25, 383–384.
- Fogel, R.A., Hess, P.C., and Rutherford, M.J. (1989) Intensive parameters of enstatite chondrite metamorphism. *Geochimica et Cosmochimica Acta*, 53, 2735–2746.
- Grady, M.M., Wright, I.P., Carr, L.P., and Pillinger, C.T. (1986) Compositional differences in enstatite chondrites based on carbon and nitrogen stable isotope measurements. *Geochimica et Cosmochimica Acta*, 50, 2799–2813.
- Herndon, J.M. and Suess, H.E. (1976) Can enstatite meteorites form in a nebula of solar composition? *Geochimica et Cosmochimica Acta*, 40, 395–399.
- Keil, K. (1968) Mineralogical and chemical relationships among enstatite chondrites. *Journal of Geophysical Research*, 73, 6945–6976.
- Keil, K. and Andersen, C.A. (1965a) Occurrences of sinoite, $\text{Si}_2\text{N}_2\text{O}$, in meteorites. *Nature*, 207, 745.
- (1965b) Electron microprobe study of the Jajh deh Kot Lalu enstatite chondrite. *Geochimica et Cosmochimica Acta*, 29, 621–632.
- Kinsey, L.K., McCoy, T.J., Keil, K., Bogard, D.D., Garrison, D.H., Kehm, K., Brazzle, R.H., Hohenberg, C.M., Mittlefehldt, D.W., and Casanova, I. (1995) Petrology, chemistry and chronology of an impact-melt clast in the Hvittis EL6 chondrite (abstract). *Lunar and Planetary Science*, 26, 753–754.
- Kornprobst, J., Pineau, F., Degiovanni, R., and Dautria, J.M. (1987) Primary igneous graphite in ultramafic xenoliths: I. Petrology of the cumulate suite in alkali basalt near Tissemt (Eggers, Algerian Sahara). *Journal of Petrology*, 28, 293–311.
- Kung, C.-C. and Clayton, R.N. (1978) Nitrogen abundances and isotopic compositions in stony meteorites. *Earth and Planetary Science Letters*, 38, 421–435.
- Lacroix, A. (1905) Matériaux sur les météorites pierreuses; 1. Identité de composition des météorites de Pillistfer (1863) et de Hvittis (1901). *Bulletin de la Société Française de Minéralogie*, 28, 70–76.
- Larimer, J.W. and Bartholomay, M. (1979) The role of carbon and oxygen in cosmic gases: Some applications to the chemistry and mineralogy of enstatite chondrites. *Geochimica et Cosmochimica Acta*, 43, 1455–1466.
- Lee, M.R., Russell, S.S., Arden, J.W., and Pillinger, C.T. (1995) Nierite (Si_3N_4), a new mineral from ordinary and enstatite chondrites. *Meteoritics*, 30, 387–398.
- Lin, Y.T., Nagel, H.-J., Lundberg, L.L., and El Goresy, A. (1991) MAC88136—The first EL3 chondrite (abstract). *Lunar and Planetary Science*, 22, 811–812.
- McBride, K. and Mason, B. (1996) Description of QUE94368. *Antarctic Meteorite Newsletter*, 19, no. 1, 16.
- McCoy, T.J., Keil, K., Bogard, D.D., Garrison, D.H., Casanova, I., Lindstrom, M.M., Brearley, A.J., Kehm, K., Nichols, R.H., Jr., and Hohenberg, C.M. (1995) Origin and history of impact-melt rocks of enstatite chondrite parentage. *Geochimica et Cosmochimica Acta*, 59, 161–175.
- Moore, C.B., Gibson, E.K., and Keil, K. (1969) Nitrogen abundances in enstatite chondrites. *Earth and Planetary Science Letters*, 6, 457–460.
- Muenow, D.W., Keil, K., and Wilson, L. (1992) High-temperature mass spectrometric degassing of enstatite chondrites: Implications for pyroclastic volcanism on the aubrite parent body. *Geochimica et Cosmochimica Acta*, 56, 4267–4280.
- Olsen, E.J., Huss, G.I., and Jarosewich, E. (1988) The Eagle, Nebraska, enstatite chondrite. *Meteoritics*, 23, 379–380.
- Petaev, M.I. and Khodakovskiy, I.L. (1986) Thermodynamic properties and conditions of formation of minerals in enstatite meteorites. In S.K. Saxena, Ed., *Chemistry and Physics of Terrestrial Planets*, p. 106–135. Springer-Verlag, New York.
- Prinz, M., Nehru, C.E., Weisberg, M.K., and Delaney, J.S. (1984) Type 3 enstatite chondrites: A newly recognized group of unequilibrated enstatite chondrites (UEC's) (abstract). *Lunar and Planetary Science*, 15, 653–654.
- Rubin, A.E. (1983a) Impact melt-rock clasts in the Hvittis enstatite chondrite breccia: Implications for a genetic relationship between EL chondrites and aubrites. Proceedings of the Lunar and Planetary Science Conference, 14th, B293–B300.
- (1983b) The Atlanta enstatite chondrite breccia. *Meteoritics*, 18, 113–121.
- (1984) The Blithfield meteorite and the origin of sulfide-rich, metal-poor clasts and inclusions in brecciated enstatite chondrites. *Earth and Planetary Science Letters*, 67, 273–283.
- (1992) A shock-metamorphic model for silicate darkening and compositionally variable plagioclase in CK and ordinary chondrites. *Geochimica et Cosmochimica Acta*, 56, 1705–1714.
- Rubin, A.E. and Grossman, J.N. (1987) Size frequency distributions of EH3 chondrules. *Meteoritics*, 22, 237–251.
- Rubin, A.E. and Scott, E.R.D. (1997) Abee and related EH chondrite impact-melt breccias. *Geochimica et Cosmochimica Acta*, 61, 425–435.
- Rubin, A.E., Scott, E.R.D., and Keil, K. (1997) Shock metamorphism of enstatite chondrites. *Geochimica et Cosmochimica Acta*, 61, 847–858.
- Ryall, W.R. and Muan, A. (1969) Silicon oxynitride stability. *Science*, 165, 1363–1364.
- Satterwhite, C. and Mason, B. (1992) Description of LEW88714. *Antarctic Meteorite Newsletter*, 15, no. 1, 17.
- Schwarz, C. and Mason, B. (1983) Description of ALHA81021. *Antarctic Meteorite Newsletter*, 6, no. 1, 12.
- (1987) Description of ALH83018. *Antarctic Meteorite Newsletter*, 10, no. 2, 16.
- (1992) Description of EET90102. *Antarctic Meteorite Newsletter*, 15, no. 2, 27.
- Score, R. and Mason, B. (1987) Description of ALH85119. *Antarctic Meteorite Newsletter*, 10, no. 2, 21.
- Sears, D.W. (1980) Formation of E chondrites and aubrites—A thermodynamic model. *Icarus*, 43, 184–202.
- Spry, A. (1969) *Metamorphic Textures*, 350 p. Pergamon, Oxford, U.K.
- Thiemens, M.H. and Clayton, R.N. (1983) Nitrogen contents and isotopic ratios of clasts from the enstatite chondrite Abee. *Earth and Planetary Science Letters*, 62, 165–168.
- Treiman, A.H. and Berkley, J.L. (1994) Igneous petrology of the new ureilites Nova 001 and Nullarbor 010. *Meteoritics*, 29, 843–848.
- Wasson, J.T., Kallemeyn, G.W., and Rubin, A.E. (1994) Equilibration temperatures of EL chondrites: A major downward revision in the ferrosilite contents of enstatite. *Meteoritics*, 29, 658–662.

MANUSCRIPT RECEIVED JANUARY 22, 1997

MANUSCRIPT ACCEPTED MAY 13, 1997